

# Spurious caustics of *Dispersion Relation Preserving* schemes

Claire David \*, Pierre Sagaut \*

\*Université Pierre et Marie Curie-Paris 6  
Institut Jean Le Rond d'Alembert, UMR CNRS 7190  
Boîte courrier n<sup>o</sup>162, 4 place Jussieu, F-75252 Paris cedex 05, France

November 1, 2018

## Abstract

A linear dispersive mechanism leading to a burst in the  $L_\infty$  norm of the error in numerical simulation of polychromatic solutions is identified. This local error pile-up corresponds to the existence of spurious caustics, which are allowed by the dispersive nature of the numerical error. From the mathematical point of view, spurious caustics are related to extrema of the numerical group velocity and are physically associated to interactions between rays defined by the characteristic lines of the discrete system. This paper extends our previous work about classical schemes to dispersion-relation preserving schemes.

*Keywords:* Dispersion; numerical schemes; spurious caustics.

## 1 Introduction

The analysis and the control of numerical error in discretized propagation-type equations is of major importance for both theoretical analysis and practical applications. A huge amount of works has been devoted to the analysis of the numerical errors, its dynamics and its influence on the computed solution (the reader is referred to classical books, among which [5, 13, 8, 9]). The emergence of *Dispersion-Relation-Preserving (DRP)* schemes [3]), which have the same dispersion relation as the original partial difference equations, enables one to have very accurate high order finite difference schemes.

The two sources of numerical error are the dispersive and dissipative properties of the numerical scheme, which are very often investigated in unbounded or periodic domains thanks to a spectral analysis.

It appears that existing works are mostly devoted to linear, one-dimensional numerical models, such as the linear advection equation

$$\frac{\partial u}{\partial t} + c \frac{\partial u}{\partial x} = 0 \quad (1)$$

where  $c$  is a constant uniform advection velocity.

The two sources of numerical error are the dispersive and dissipative properties of the numerical scheme, which are very often investigated in unbounded or periodic domains thanks to a spectral analysis. Following this approach, a monochromatic wave is used to measure the accuracy of the scheme. Such a tool is very powerful and provides the user with a deep insight into the discretization errors. But some results coming from practical numerical experiments still remain unexplained, despite the linear character of the discrete numerical model. As an example, let us note the sudden growth of the numerical error for long range propagation reported by Zingg [15] for a large set of numerical schemes, including optimized numerical schemes.

The usual modal analysis is almost always applied to monochromatic reference solutions, with the purpose of analyzing the error committed on both their amplitude and their phase, leading to classical plots of the relative error as the function of the Courant number and/or the number of grid points per wavelength. Therefore, dispersive phenomena associated to polychromatic solutions are usually not taken into account.

The present paper deals with the analysis of linear dispersive mechanism which results in local error focusing, i.e. to a sudden local error burst in the  $L_\infty$  norm for polychromatic solutions. This phenomena is reminiscent of the physical one referred to as the caustic phenomenon in linear dispersive physical models [14], and will be referred to as the spurious caustic phenomenon hereafter. It extends our previous work [2] to *DRP* schemes. The present analysis is restricted to interior stencil, and the influence of boundary conditions will not be considered. The paper is organized as follows. Main elements of caustic theory of interest for the present analysis are recalled in section 2. *DRP* schemes are presented in section 3. Their caustical analysis is exposed in section 4. A numerical example is presented in section 5.

## 2 Caustics

The solution of Eq. (1) is taken under the form:

$$u(x, t, k) = e^{i(kx - \omega t)} \quad (2)$$

where  $\omega = \xi_\omega + i\eta_\omega$  is the complex phase, and  $k$  the real wave number. For dispersive waves, it is recalled that the group velocity  $V_g(k)$  is defined as

$$V_g(k) \equiv \frac{\partial \xi_\omega}{\partial k} \quad (3)$$

A caustic is defined as a focusing of different rays in a single location. The equivalent condition is that the group velocity exhibits an extremum, i.e. there exists at least one wave number  $k_c$  such that

$$\frac{\partial V_g}{\partial k}(k_c) = 0 \quad (4)$$

The corresponding physical interpretation is that wave packets with characteristic wave numbers close to  $k_c$  will pile-up after a finite time and will remain superimposed for a long time, resulting in the existence a region of high energy followed by a region with very low fluctuation level.

The linear continuous model Eq. (1) is not dispersive if the convection velocity  $c$  is uniform, and therefore the exact solution does not exhibit caustics since the group velocity does not depend on  $k$ . The discrete solution associated with a given numerical scheme will admit spurious caustics, and therefore spurious local energy pile-up and local sudden growth of the error, if the discrete dispersion relation is such that the condition (4) is satisfied. For a uniform scale-dependent convection velocity, such spurious caustics can exist in polychromatic solutions only, since they are associated to the superposition of wave packets with different characteristic wave numbers.

Set:

$$k = \frac{\varphi \sigma}{c dt} \quad (5)$$

The general dispersion relation associated with the discrete scheme enables us to obtain the corresponding group velocity, given by:

$$V_g = h \frac{\partial \xi_\omega}{\partial \varphi} \quad (6)$$

The numerical solution will therefore admits spurious caustics if

$$\frac{\partial V_g}{\partial k} = \frac{\partial V_g}{\partial \varphi} \frac{\partial \varphi}{\partial k} = 0 \iff \frac{\partial V_g}{\partial \varphi} = 0 \quad (7)$$

The corresponding values of  $\varphi$  and  $k$  will be respectively denoted  $\varphi_c$  and  $k_c$ . Spurious caustics are associated with characteristic lines given by

$$\frac{x}{t} = U_c \quad (8)$$

where

$$U_c = V_g(\varphi_c) \quad (9)$$

### 3 *DRP* schemes

The Burgers equation:

$$u_t + c u u_x - \mu u_{xx} = 0, \quad (10)$$

$c, \mu$  being real constants, plays a crucial role in the history of wave equations. It was named after its use by Burgers [1] for studying turbulence in 1939.

$i, n$  denoting natural integers, a linear finite difference scheme for this equation can be written under the form:

$$\sum \alpha_{lm} u_l^m = 0 \quad (11)$$

where:

$$u_l^m = u(lh, m\tau) \quad (12)$$

$l \in \{i-1, i, i+1\}$ ,  $m \in \{n-1, n, n+1\}$ ,  $j = 0, \dots, n_x$ ,  $n = 0, \dots, n_t$ . The  $\alpha_{lm}$  are real coefficients, which depend on the mesh size  $h$ , and the time step  $\tau$ . The Courant-Friedrichs-Lewy number ( $cfl$ ) is defined as  $\sigma = c\tau/h$ .

A numerical scheme is specified by selecting appropriate values of the coefficients  $\alpha_{lm}$ . Then, depending on them, one can obtain optimum schemes, for which the error will be minimal.

$m$  being a strictly positive integer, the first derivative  $\frac{\partial u}{\partial x}$  is approximated at the  $l^{th}$  node of the spatial mesh by:

$$\left(\frac{\partial u}{\partial x}\right)_l \simeq \sum_{k=-m}^m \gamma_k u_{i+k}^n \quad (13)$$

Following the method exposed by C. Tam and J. Webb in [3], the coefficients  $\gamma_k$  are determined requiring the Fourier Transform of the finite difference scheme (13) to be a close approximation of the partial derivative  $\left(\frac{\partial u}{\partial x}\right)_l$ . (13) is a special case of:

$$\left(\frac{\partial u}{\partial x}\right)_l \simeq \sum_{k=-m}^m \gamma_k u(x + kh) \quad (14)$$

where  $x$  is a continuous variable, and can be recovered setting  $x = lh$ . Denote by  $\omega$  the phase. Applying the Fourier transform, referred to by  $\hat{\cdot}$ , to both sides of (14), yields:

$$j\omega \hat{u} \simeq \sum_{k=-m}^m \gamma_k e^{jk\omega h} \hat{u} \quad (15)$$

$j$  denoting the complex square root of  $-1$ .

Comparing the two sides of (15) enables us to identify the wavenumber  $\bar{\lambda}$  of the finite difference scheme (13) and the quantity  $\frac{1}{j} \sum_{k=-m}^m \gamma_k e^{jk\omega h}$ , the wavenumber of the finite difference scheme (13) is thus:

$$\bar{\lambda} = -j \sum_{k=-m}^m \gamma_k e^{j k \omega h} \quad (16)$$

To ensure that the Fourier transform of the finite difference scheme is a good approximation of the partial derivative  $(\frac{\partial u}{\partial x})_l$  over the range of waves with wavelength longer than  $4h$ , the a priori unknowns coefficients  $\gamma_k$  must be chosen so as to minimize the integrated error:

$$\begin{aligned} \mathcal{E} &= \int_{-\frac{\pi}{2}}^{\frac{\pi}{2}} |\lambda h - \bar{\lambda} h|^2 d(\lambda h) \\ &= \int_{-\frac{\pi}{2}}^{\frac{\pi}{2}} |\lambda h + j \sum_{k=-m}^m \gamma_k e^{j k \omega h} h|^2 d(\lambda h) \\ &= \int_{-\frac{\pi}{2}}^{\frac{\pi}{2}} |\zeta + j \sum_{k=-m}^m \gamma_k \{\cos(k \zeta) + j \sin(k \zeta)\}|^2 d\zeta \\ &= \int_{-\frac{\pi}{2}}^{\frac{\pi}{2}} \left\{ \left[ \zeta - \sum_{k=-m}^m \gamma_k \sin(k \zeta) \right]^2 + \left[ \sum_{k=-m}^m \gamma_k \cos(k \zeta) \right]^2 \right\} d\zeta \\ &= 2 \int_0^{\frac{\pi}{2}} \left\{ \left[ \zeta - \sum_{k=-m}^m \gamma_k \sin(k \zeta) \right]^2 + \left[ \sum_{k=-m}^m \gamma_k \cos(k \zeta) \right]^2 \right\} d\zeta \end{aligned} \quad (17)$$

The conditions that  $\mathcal{E}$  is a minimum are:

$$\frac{\partial \mathcal{E}}{\partial \gamma_i} = 0, \quad i = -m, \dots, m \quad (18)$$

i. e.:

$$\int_0^{\frac{\pi}{2}} \left\{ -\zeta \sin(i \zeta) + \sum_{k=-m}^m \gamma_k \cos((k-i) \zeta) \right\} d\zeta = 0 \quad (19)$$

Changing  $i$  into  $-i$ , and  $k$  into  $-k$  in the summation yields:

$$\int_0^{\frac{\pi}{2}} \left\{ \zeta \sin(i \zeta) + \sum_{k=-m}^m \gamma_{-k} \cos((-k+i) \zeta) \right\} d\zeta = 0 \quad (20)$$

i. e.:

$$\int_0^{\frac{\pi}{2}} \left\{ \zeta \sin(i \zeta) + \sum_{k=-m}^m \gamma_{-k} \cos((k-i) \zeta) \right\} d\zeta = 0 \quad (21)$$

Thus:

$$\int_0^{\frac{\pi}{2}} \sum_{k=-m}^m \{\gamma_{-k} + \gamma_k\} \cos((k-i) \zeta) d\zeta = 0 \quad (22)$$

which yields:

$$\frac{\pi}{2} \{\gamma_{-i} + \gamma_i\} + \sum_{k \neq i, k=-m}^m \left\{ \frac{\gamma_{-k} + \gamma_k}{k-i} \right\} \sin\left((k-i) \frac{\pi}{2}\right) = 0 \quad (23)$$

which can be considered as a linear system of  $2m + 1$  equations, the unknowns of which are the  $\gamma_{-i} + \gamma_i$ ,  $i = -m, \dots, m$ . The determinant of this system is not equal to zero, while it is the case of its second member: the Cramer formulae give then, for  $i = -m, \dots, m$ :

$$\gamma_{-i} + \gamma_i = 0 \quad (24)$$

or:

$$\gamma_{-i} = -\gamma_i \quad (25)$$

For  $i = 0$ , one of course obtains:

$$\gamma_0 = 0 \quad (26)$$

All this ensures:

$$\sum_{k=-m}^m \gamma_k = 0 \quad (27)$$

The values of the  $\gamma_k$  coefficients are obtained by substituting relations (25) into (19):

$$\sum_{k=-m}^m \gamma_k = 0 \quad (28)$$

$m$  being a strictly positive integer, a  $2m + 1$ -points *DRP* scheme ([3]) is thus given by:

$$-u_i^{n+1} + u_i^n + \frac{\tau}{h} \sum_{k=-m}^m \gamma_k u_{i+k}^n = 0 \quad (29)$$

where the  $\gamma_k$ ,  $k \in \{-m, m\}$  are the coefficients of the considered scheme, and satisfy the relations (25).

## 4 General study of *DRP* schemes

The dispersion relation related to a general *DRP*-scheme (29) is given by:

$$\frac{\tau}{h} \sum_{k=-m}^m \gamma_k e^{i(k\varphi + \xi\omega\tau) - B\tau + e^{i\xi\omega\tau} \tau - B\tau} - 1 = 0 \quad (30)$$

from which it comes that

$$i\xi\omega\tau = B\tau - \ln \left( 1 + \frac{\tau \sum_{k=-m}^m \gamma_k e^{ik\varphi}}{h} \right) \quad (31)$$

The group velocity can be expressed as

$$V_g = \frac{i \sum_{k=-m}^m i k \gamma_k e^{i k \varphi}}{\omega \left( \frac{\sigma \sum_{k=-m}^m \gamma_k e^{i k \varphi}}{c} + 1 \right)} \quad (32)$$

from which it comes that

$$\frac{\partial V_g}{\partial \varphi} = \frac{i c^2 \tau \left( \left( c + \sigma \sum_{k=-m}^m \gamma_k e^{i k \varphi} \right) \sum_{k=-m}^m i k^2 \gamma_k e^{i k \varphi} - \sigma \left( \sum_{k=-m}^m \gamma_k e^{i k \varphi} i k \right)^2 \right)}{\sigma \left( c + \sigma \sum_{k=-m}^m \gamma_k e^{i k \varphi} \right)^2} \quad (33)$$

Through identification of the real and imaginary part of (33), we obtain:

$$\sigma \sum_{k,l=-m}^m \gamma_k \gamma_{i+l} \{k^2 \sin[(k+l)\varphi] - k l \cos[(k+l)\varphi]\} = -c \sum_{k=-m}^m k^2 \gamma_k \sin(k\varphi) \quad (34)$$

and

$$\sigma \sum_{k,l=-m}^m \gamma_k \gamma_l \{-\cos[(k+l)\varphi] - k l \sin[(k+l)\varphi]\} = c \sum_{k=-m}^m k^2 \gamma_k \cos(k\varphi) \quad (35)$$

Due to (25), (36) and (37) respectively become:

$$\sigma \sum_{k,l=-m}^m \gamma_k \gamma_l \{k^2 \sin[(k+l)\varphi] - k l \cos[(k+l)\varphi]\} = -2c \sum_{k=1}^m k^2 \gamma_k \sin(k\varphi) \quad (36)$$

and

$$\sigma \sum_{k,l=-m}^m \gamma_k \gamma_l \{-\cos[(k+l)\varphi] - k l \sin[(k+l)\varphi]\} = 0 \quad (37)$$

Denote by  $T_j$ ,  $j \in \mathbb{N}^*$  the Chebyshev polynomial of the first kind, and by  $U_j$ ,  $j \in \mathbb{N}^*$  the Chebyshev polynomial of the second kind:

$$\cos(jx) = T_j(\cos(x)) = \frac{n}{2} \sum_{k=0}^{\lfloor \frac{n}{2} \rfloor} (-1)^k \frac{(n-k-1)!}{k!(n-2k)!} (2 \cos(x))^{n-2k} \quad (38)$$

$$\sin(jx) = \sin(x) U_j(\cos(x)) \quad (39)$$

where:

$$U_j(\cos(x)) = \sum_{k=0}^{\lfloor \frac{n}{2} \rfloor} (-1)^k \frac{(n-k)!}{k!(n-2k)!} (2 \cos(x))^{n-2k} \quad (40)$$

$\left[\frac{n}{2}\right]$  denotes the integer part of  $\frac{n}{2}$ .

Equations (36), (37) can thus be written as:

$$\sigma \sum_{k,l=-m}^m \gamma_k \gamma_l \{k^2 \sin(\varphi) U_{k+l}(\cos(\varphi)) - k l T_{k+l}(\cos(\varphi))\} = -c \sum_{k=-m}^m k^2 \gamma_k \sin(\varphi) U_k(\cos(\varphi)) \quad (41)$$

and

$$\sigma \sum_{k,l=-m}^m \gamma_k \gamma_l \{T_{k+l}(\cos(\varphi)) + k l \sin(\varphi) U_{k+l}(\cos(\varphi))\} = 0 \quad (42)$$

Using the relation:

$$\sin(\varphi) = \sqrt{1 - \cos^2(\varphi)} \quad (43)$$

equations (41), (42) can be written as:

$$f_1(\cos(\varphi)) = 0 \quad (44)$$

and

$$f_2(\cos(\varphi)) = 0 \quad (45)$$

where, for all  $\theta \in \mathbb{R}$ :

$$f_1(\theta) = \sigma \sum_{k,l=-m}^m \gamma_k \gamma_l \{k^2 \sqrt{1 - \theta^2} U_{k+l}(\theta) - k l T_{k+l}(\theta)\} + c \sum_{k=-m}^m k^2 \gamma_k \sqrt{1 - \theta^2} U_k(\theta) \quad (46)$$

i.e.:

$$f_1(\theta) = \sigma \sum_{k,l=-m}^m \gamma_k \gamma_l \{k^2 \sqrt{1 - \theta^2} U_{k+l}(\theta) - k l T_{k+l}(\theta)\} + 2c \sum_{k=1}^m k^2 \gamma_k \sqrt{1 - \theta^2} U_k(\theta) \quad (47)$$

and

$$f_2(\theta) = \sum_{k,l=-m}^m \gamma_k \gamma_l \{T_{k+l}(\theta) + k l \sqrt{1 - \theta^2} U_{k+l}(\theta)\} \quad (48)$$

Due to:

$$T_j(1) = 1 \quad \forall j \in \mathbb{N}^* \quad (49)$$

it is worth noting that:

$$f_1(1) = -\sigma \sum_{k,l=-m}^m \gamma_k \gamma_l k l \quad (50)$$

and

$$f_2(1) = \sum_{k,l=-m}^m \gamma_k \gamma_l \quad (51)$$



The knowledge of the scheme coefficients  $\gamma_k$ ,  $k \in \{-m, m\}$ , enables one to study their variations, and to determine whether the equations (44), (45) admit a solution. One can thus know whether  $\frac{\partial V_g}{\partial \varphi} = 0$  admits real roots, i. e. whether the schema has spurious caustics.

## 5 Numerical application: the 3-points DRP scheme

The 3-points DRP scheme is given by:

$$\gamma_1 = 0.63662 \quad (52)$$

We thus have:

$$f_1(1) = -2\sigma \{\gamma_1^2 - \gamma_1^2\} = 0 \quad (53)$$

and

$$f_2(1) = 2 \{\gamma_1^2 - \gamma_1^2\} = 0 \quad (54)$$

For the 3-points DRP scheme, the dispersion relation is:

$$e^{i\varphi} \left( -e^{-\eta\omega\tau} + e^{i\tau\xi\omega} \right) + e^{i\tau\xi\omega} \left( -0.63662 + 0.63662 e^{2i\varphi} \right) \sigma = 0 \quad (55)$$

which leads to:

$$e^{i\tau\xi\omega} = \frac{e^{i\varphi} e^{-\eta\omega\tau}}{e^{i\varphi} + 0.63662\sigma(e^{2i\varphi} - 1)} \quad (56)$$

It yields:

$$\xi\omega = \frac{1}{\tau} \text{Arctan} \left[ \frac{-(1 + 0.63662\sigma) \sin(\varphi)}{1 + (0.63662\sigma - 1) \cos(\varphi)} \right] \quad (57)$$

The derivative  $\frac{\partial V_g}{\partial \varphi}$  of the group velocity  $V_g$  vanishes for  $\varphi = 0$ ,  $\varphi = \frac{\pm\pi}{2}$ , and  $\varphi = 0.950935$ .

The 3-points DRP scheme admits thus spurious caustics.

We now illustrate the caustic phenomenon considering the two following sinusoidal wave packets:

$$u_1 = e^{-\alpha(x-x_0^1-ct)^2} \text{Cos}[k_1(x-x_0^1-ct)] \quad (58)$$

$$u_2 = e^{-\alpha(x-x_0^2-ct)^2} \text{Cos}[k_2(x-x_0^2-ct)] \quad (59)$$

where  $\alpha > 0$ . The two wave packets are initially centered at  $x_0^1$  and  $x_0^2$ , respectively. The group velocity of the two wave packets are  $V_1 = V_g(k_1)$  and  $V_2 = V_g(k_2)$ , respectively, where the function  $V_g(x)$  is associated to the numerical scheme used to solve Eq. (1).

If the solution obeys the linear advection law given by Eq. (1), the initial field is passively advected at speed  $c$ , while, if the advection speed is scale-dependent (as

in numerical solutions), the two packets will travel at different speeds, leading to the rise of discrepancies with the constant-speed solution. Another dispersive error is the shape-deformation phenomenon: due to numerical errors, the exact shape of the wave packets will not be exactly preserved. This secondary effect will not be considered below, since it is not related to the existence of spurious caustics. It is emphasized here that the occurrence of spurious caustics originates in the differential error in the group velocity, not in the fact that shapes of the envelope of the wave packets are not preserved. The issue of deriving shape-preserving schemes for passive scalar advection has been addressed by several authors (e.g. [6, 7]).

The spurious caustics will appear if the two wave packets happen to get superimposed. During the cross-over, the  $L_\infty$  norm of the error (defined as the difference between the constant-speed solution and the dispersive one) will exhibit a maximum. The characteristic life time of the caustic,  $t^*$ , depends directly on the difference between the advection speeds of the two wave packets and the wave packet widths. Denoting  $l_1$  and  $l_2$  the characteristic length of the two wave packets, the time during which they will be (at least partially) superimposed can be estimated as

$$t^* = \frac{l_1 + l_2}{|V_1 - V_2|} \quad (60)$$

It is seen that, since caustics are defined as solutions for which  $\partial V_g / \partial k = 0$ ,  $t^*$  will be large if  $|k_1 - k_2| \ll 1$ . Noting  $k_1 = k_c + \delta k$  and  $k_2 = k_c - \delta k$ , one obtains

$$t^* \simeq \frac{l_1 + l_2}{2(\delta k)^2 \left| \frac{\partial^2 V_g}{\partial k^2}(k_c) \right|} \quad (61)$$

leading to  $t^* \propto (\delta k)^{-2}$ .

Neglecting shape-deformation effects and assuming that the numerical scheme is non-dissipative, the numerical error  $E$  is given by:

$$E = |e^{-\alpha(x-x_0^1-ct)^2} \text{Cos}[k_1(x-x_0^1-ct)] - e^{-\alpha(x-x_0^1-tV_1)^2} \text{Cos}[k_1(x-x_0^1-tV_1)] \\ + e^{-\alpha(x-x_0^2-ct)^2} \text{Cos}[k_2(x-x_0^2-ct)] - e^{-\alpha(x-x_0^2-tV_2)^2} \text{Cos}[k_2(x-x_0^2-tV_2)]| \quad (62)$$

A simple analysis show that

$$\lim_{t \rightarrow +\infty} L_\infty(E(t)) = L_\infty(u_1(t=0)), \quad \max_t L_\infty(E(t)) = 2L_\infty(u_1(t=0)) \quad (63)$$

The time history of the  $L_\infty$  norm of  $E$  for the 3-points *DRP* scheme scheme, is displayed in Fig. 1, showing the occurrence of the caustic and the sudden growth of the  $L_\infty$  error norm.

Figure 2 displays the isovalues of the residual kinetic energy for 3-points *DRP* scheme, for  $cf l = 0.9$ . Minima are in black, maxima in white. In each case, the caustic corresponds to the white domain, where the residual kinetic energy is maximal.

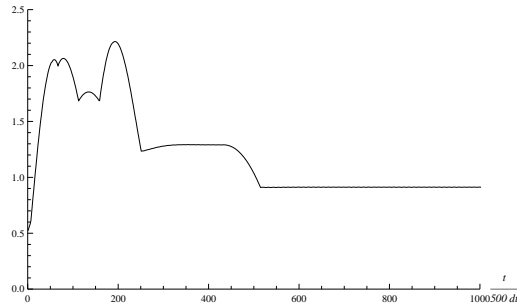


Figure 1: Time history ( $L_\infty$  norm) of the numerical error for the two-wave packet problem (shape deformation and dissipative errors are neglected to emphasize the linear focusing phenomenon). Numerical parameters are  $\alpha = 0.0005$ ,  $h = 0.01$ ,  $V_1 = -2.68381$ ,  $V_2 = -2.51381$ , corresponding to the properties of the 3-points *DRP* scheme, for  $\sigma = 0.9$ .

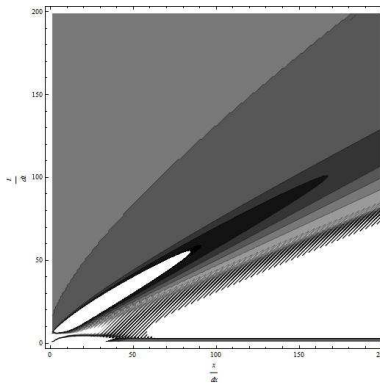


Figure 2: Isovalues of the residual kinetic energy for the 3-points *DRP* scheme, for  $cf l = 0.9$ .

## 6 Concluding remarks

In the above, we have set a general method that enables one to determine whether a *DRP* scheme admits or not spurious caustics.

The existence of spurious numerical caustics in linear advection *DRP* schemes has been proved. This linear dispersive phenomenon gives rise to a sudden growth of the  $L_\infty$  norm of the error, which corresponds to a local focusing of the numerical error in both space and time. In the present analysis, spurious caustics have been shown to occur in polychromatic solutions. The energy of the caustic phenomenon depends on the number of spectral modes that will get superimposed at the same time. As a consequence, the spurious error pile-up will be more pronounced in simulations with very small wave-number increments. It has been shown that a popular existing scheme, as the 3-points *DRP*-scheme,

allows the existence of spurious caustics.

## References

- [1] Burgers J. M., Mathematical examples illustrating relations occurring in the theory of turbulent fluid motion, *Trans. Roy. Neth. Acad. Sci.* Amsterdam, 17 (1939) 1-53.
- [2] Cl. David, P. Sagaut, T. Sengupta, *A linear dispersive mechanism for numerical error growth: spurious caustics*, European Journal of Fluid Mechanics, under press.
- [3] C.K. Tam, J.C. Webb, *Dispersion-Relation-Preserving Finite Difference schemes for Computational Acoustics*, Journal of Computational Physics, 107 (1993), 262-281.
- [4] D. Bouche, G. Bonnaud, D. Ramos, Comparison of numerical schemes for solving the advection equation, *Applied Math Letters* 16 (2003).
- [5] C. Hirsch, *Numerical Computation of Internal and External Flows*, Wiley-Interscience (1988).
- [6] B.P. Leonard, A.P. Lock, M.K. Macvean, The NIRVANA scheme applied to one-dimensional advection, *Int. J. Num. Meth. Heat Fluid Flow* 5 (1995) 341-377.
- [7] B.P. Leonard, A.P. Lock, M.K. Macvean, Conservative explicit unrestricted-time-step multidimensional constancy-preserving advection schemes, *Monthly Weather Review* 124 (1996) 2588-2606.
- [8] H. Lomax, T.H. Pulliam, D.W. Zingg, *Fundamentals of Computational Fluid Dynamics*, Springer (2002).
- [9] T.K. Sengupta, *Fundamentals of Computational Fluid Dynamics*, Hyderabad Univ. Press (2004).
- [10] T.K. Sengupta, A. Dipankar, A comparative study of time advancement methods for solving Navier-Stokes equations, *J. Sci. Comput.* 21 (2004), no. 2, 225-250.
- [11] T.K. Sengupta, S.K. Sircar, A. Dipankar, High accuracy schemes for DNS and acoustics, *J. Sci. Comput.* 26(2) (2006) 151-193.
- [12] T.K. Sengupta, A. Dipankar, P. Sagaut, A Fourier-Laplace spectral theory of computing for non-periodic problems: signal and error propagation dynamics. Submitted
- [13] R. Vichnevetsky, J.B. Bowles, *Fourier Analysis of Numerical Approximations of Hyperbolic Equations*, SIAM Stud. Appl. Math. 5 (1982).

- [14] G.B. Witham, *Linear and Nonlinear Wave*, Wiley-Interscience (1974).
- [15] D.W. Zingg, Comparison of high-accuracy finite-difference methods for linear wave propagation, *SIAM J. Sci. Comput.* 22 (2000) 227-238.